Solid State Communications 149 (2009) 1140–1143

Contents lists available at ScienceDirect

Solid State Communications

journal homepage: www.elsevier.com/locate/ssc

Gauge fields, ripples and wrinkles in graphene layers

F. Guinea [a,*], Baruch Horovitz [b], P. Le Doussal [c]

[a] *Instituto de Ciencia de Materiales de Madrid, CSIC, Cantoblanco, E-28049 Madrid, Spain*

[b] *Department of Physics, Ben Gurion University, Beer Sheva 84105, Israel*

[c] *CNRS-Laboratoire de Physique Théorique de l'Ecole Normale Supérieure, 24 rue Lhomond, 75231 Cedex 05, Paris, France*

ARTICLE INFO

Article history:
Received 7 November 2008
Received in revised form
2 February 2009
Accepted 2 February 2009 by the Guest Editors
Available online 20 March 2009

PACS:
73.20.-r
73.20.Hb
73.23.-b
73.43.-f

Keywords:
A. Graphene
A. Membrane
D. Ripples
D. Deformation

ABSTRACT

We analyze elastic deformations of graphene sheets which lead to effective gauge fields acting on the charge carriers. Corrugations in the substrate induce stresses which, in turn, can give rise to mechanical instabilities and the formation of wrinkles. Similar effects may take place in suspended graphene samples under tension.

1. Introduction

Two dimensional graphene membranes define a new class of materials with a number of novel and promising features [1–3]. From a basic point of view, one of the striking properties of graphene is that many types of long wavelength disorder influence the electrons as effective gauge fields [4–15], which modify the electronic properties, as measured, for instance, in weak localization experiments [7,8,16,17].

Because of the existence of two inequivalent valleys in the Brillouin Zone of graphene, one can formally define two types of gauge fields, one of which induces mixing between the valleys, and another which does not. These two fields do not commute. A gauge field which effectively rotates electrons from one valley into electrons in the other valley is needed to describe lattice disclinations, such as pentagonal and heptagonal rings [4,5,18,19]. Intravalley gauge fields can be induced by elastic strains [7,12,20,21], by curvature [9], or by lattice defects such as dislocations. For each type of field, the Hamiltonian can be written as two independent Dirac equations, with gauge fields of opposite sign for each of them, so that it is invariant with respect to time reversal.

Elastic strains of reasonable values, $\bar{u} \sim 0.02$–0.05 with the correct symmetries can lead to significant effective magnetic fields, $B \sim 0.1$–1 T [7,12]. Large graphene sheets show corrugations [22], and significant scale deformations [23–25]. Suspended samples [25,26] can also be deflected if a gate potential is applied to them [27]. Graphene deposited on a substrate shows corrugations [24,28–30]. The existence of corrugations is confirmed by numerical simulations [31].

The low energy electronic states of graphene are described by the Dirac equation [3]. The properties of the electronic spectrum of the Dirac equation in the presence of a random gauge field has been studied in connection with the Quantum Hall Effect [32–34]. The scattering cross section of isolated ripples vanishes at short and long electron wavelengths, with a peak for wavelengths comparable to the size of the ripple [35]. The density of states is changed at low energies, and it acquires an anomalous power law dependence on energy, where the exponent depends on the strength of the disorder. The combined effect of random gauge fields and the long range electron–electron interaction leads to a complex phase diagram when the system is close to the neutrality point [36–38].

* Corresponding author.
E-mail address: paco.guinea@icmm.csic.es (F. Guinea).

0038-1098/$ – see front matter
doi:10.1016/j.ssc.2009.02.044

In the following, we discuss some basic features of ripples and wrinkles in single layer graphene. We analyze, in the following section, the elastic strains in a periodic array of ripples, similar to that reported in [39], and the effect of the induced gauge fields. We next discuss possible mechanisms which may induce wrinkles [40] in graphene, and the way they can alter the electronic properties.

We will not consider here the effect of a scalar potential also induced by the presence of strains [20]. When the length scale of the corrugations is larger than the Thomas–Fermi screening length $k_s^{-1} \sim k_F^{-1}$, where k_F is the Fermi wavevector, these scalar fields will be screened [27], while the gauge fields are not. This picture is confirmed by full electronic calculations of rippled graphene layers [14].

2. Periodic array of ripples

The simplest corrugation which leads to inhomogeneous strains and, as a result, to non trivial gauge fields in graphene is a periodic array of ripples, which can be induced by a suitable substrate [39]. For simplicity, we assume the existence of modulation of the out of plane displacement of the graphene layer of the type:

$$h(x, y) = h_0 \left[2\cos(\vec{G}_1\vec{r}) + 2\cos(\vec{G}_2\vec{r}) + 2\cos(\vec{G}_3\vec{r}) \right] \quad (1)$$

where $\vec{G}_1 = G\mathbf{n_x}$, $\vec{G}_2 = G(\mathbf{n_x}/2 + \sqrt{3}\mathbf{n_y}/2)$ and $\vec{G}_3 = G(-\mathbf{n_x}/2 + \sqrt{3}\mathbf{n_y}/2)$. These vectors define a triangular lattice. In terms of the in-plane displacements, $\vec{u}(x, y)$, the strain tensor is:

$$\begin{aligned} u_{xx} &= \partial_x u_x + \frac{(\partial_x h)^2}{2} \\ u_{yy} &= \partial_y u_y + \frac{\left(\partial_y h\right)^2}{2} \\ u_{xy} &= \frac{\partial_y u_x + \partial_x u_y}{2} + \frac{(\partial_x h)\left(\partial_y h\right)}{2}. \end{aligned} \quad (2)$$

Neglecting, for the moment, the contribution due to the bending stiffness of the graphene layer, the free energy can be written as [41]:

$$\mathcal{F} \equiv \frac{\lambda}{2} \int \mathrm{d}^2\vec{r}\, (u_{xx} + u_{yy})^2 + \mu \int \mathrm{d}^2\vec{r}\, (u_{xx}^2 + u_{yy}^2 + 2u_{xy}^2) \quad (3)$$

where, using for the longitudinal and transverse sound velocities of graphene [42–44] the values $v_L = 22.2$ km/s and $v_T = 14.7$ km/s, we find $\lambda = 1.6$ eV Å^{-2} and $\mu = 5.7$ eV Å^{-2}.

The full strain tensor u_{ij} can be obtained from the tensor $f_{ij} = (\partial_i h)\left(\partial_j h\right)$ by minimizing the free energy, Eq. (3), and obtaining the in-plane displacement field, $\vec{u}$ [13]. In terms of the strain tensor, the effective gauge field acting on the electrons, for a given valley in the Brillouin Zone, is [20,21]:

$$\begin{aligned} A_x(\vec{r}) &= \frac{c\Phi_0}{a} \frac{\partial \log(t)}{\partial \log(a)} \left(u_{xx} - u_{yy}\right) \\ A_y(\vec{r}) &= 2\frac{c\Phi_0}{a} \frac{\partial \log(t)}{\partial \log(a)} u_{xy} \end{aligned} \quad (4)$$

where $\beta = \partial \log(t)/\partial \log(a) \approx 2$ gives the dependence of the tight binding hopping element between orbitals in nearest neighbor carbon atoms, $t \approx 3$ eV, on the distance between them, $a \approx 1.4$ Å, c is a numerical constant of order unity, and Φ_0 is the quantum unit of flux. In this analysis, we have assumed that the shape of the corrugation, $h(x, y)$, is determined by external forces. We now consider the bending rigidity of the layer. From the continuum theory of elasticity [41] we expect a term:

$$\mathcal{F}_b = \frac{\kappa_1}{2} \int \mathrm{d}^2\vec{r} \left[\left(\frac{\partial^2 h}{\partial x^2} \right) + \left(\frac{\partial^2 h}{\partial y^2} \right) \right]^2 + \frac{\kappa_2}{2} \int \mathrm{d}^2\vec{r} \left[\left(\frac{\partial^2 h}{\partial x^2} \right)^2 + \left(\frac{\partial^2 h}{\partial y^2} \right)^2 + \frac{1}{2} \left(\frac{\partial^2 h}{\partial x \partial y} \right)^2 \right]. \quad (5)$$

For graphene, $\kappa_1 \sim \kappa_2 \sim \bar{\kappa} \sim 1$ eV. The ratio between the bending and compression energies of the ripples is approximately proportional to $G^2\bar{\kappa}/(\lambda + 2\mu)$. For mesoscopic ripples of lengths $l = 2\pi G^{-1} \sim 10 - 100$ nm, the bending rigidity can be neglected.

The calculation of the strain tensor and effective gauge fields for the height profile in Eq. (1) is rather simple. Values for the strain

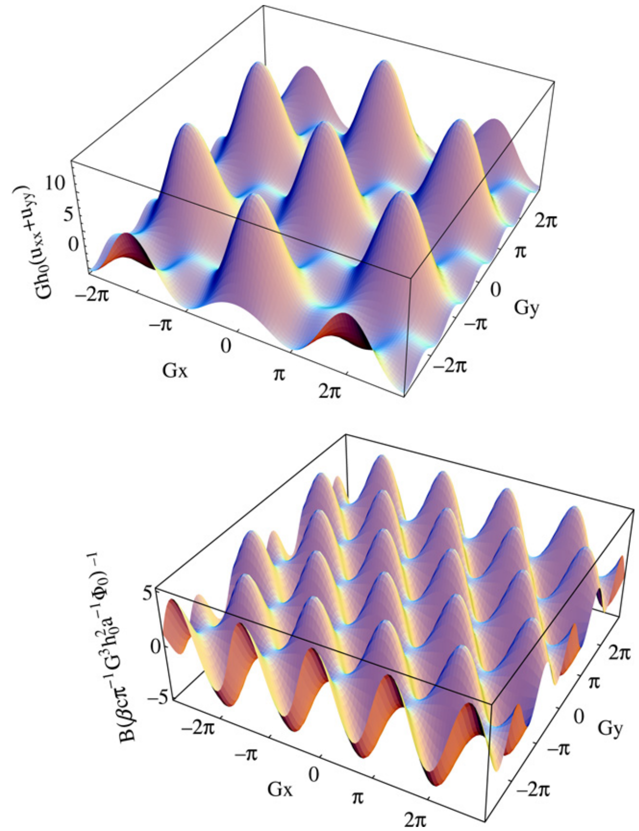

Fig. 1. (Color online). Top: Compression, $u_{xx} + u_{yy}$, induced by a periodic array of ripples, see text for details. Bottom: Effective magnetic field for the same array.

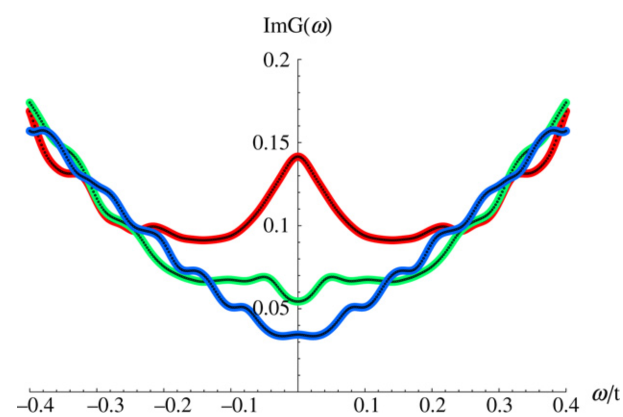

Fig. 2. (Color online). Density of states for a periodic array of ripples, including the induced gauge field. Blue: $h_0 = 0$. Green: $\frac{3c\beta aG}{2}(Gh_0)^2 = 0.025$. Red: $\frac{3c\beta aG}{2}(Gh_0)^2 = 0.05$.

Fig. 3. (Color online). Generation of wrinkles in a graphene layer on SiO_2. Top: The layer is compressed against the corrugated substrate. Bottom: When the external pressure is removed, in-plane stresses due to the deformation of the layer induce wrinkles, if the pinning to the substrate is sufficiently weak.

and induced magnetic field are shown in Fig. 1. The electronic density of states, calculated including the gauge field due to the ripples, is shown in Fig. 2. The results have been obtained by using a discrete lattice model with $2 \times 81 \times 81$ sites with a broadening of the levels of $\delta\omega = 0.03t$. The small amplitude undulations in the density of states are an artifact due to the discretization. The finite level broadening also leads to a finite density of states at the Dirac point in the absence of a gauge field.

There is a peak at the Dirac energy for the largest corrugations, consistent with analytical results for the density of states of Dirac electrons in the presence of a random gauge field [34]. Similar effects are obtained in numerical studies of the Dirac equation in a random field whose fluctuations are smooth on the scale of the lattice [45], although they have not been found if the gauge field varies on length scales comparable to the lattice spacing [33]. The highest effective magnetic fields induced by ripples with $h_0 \sim 1$ nm and $l = 2\pi G^{-1} \sim 60$ nm can be large, $B_{\max} \sim 2$–5 T [7], so that the number of flux quanta per ripple exceeds one.

3. Wrinkling of graphene layers: Graphene on a substrate

As in any membrane, topological lattice defects can spontaneously lead to corrugations [46] in graphene (see also Sec. VIB in [13]). Similar effects can be expected from impurities which induce lattice deformations [47]. Rigid layers on soft substrates show wrinkles if they are under anisotropic stresses which exceed a given threshold [40,48,49]. A related situation which may be relevant for graphene layers on SiO_2 substrates is sketched in Fig. 3. The exfoliation procedure applies pressure on the graphene layer against the corrugated substrate, inducing deformations and in-plane stresses. When the pressure is removed, the system can reduce the elastic energy by forming wrinkles, provided that the stresses are sufficiently large and the pinning energy to the substrate is sufficiently low.

We show in Fig. 4 the stresses σ_{xx} and σ_{yy} induced by the periodic array of ripples discussed in the previous section. There are regions, whose length is fraction of G^{-1}, where the stresses are highly anisotropic. The gain in elastic free energy per unit area due to the formation of wrinkles in these regions is $\mathcal{F} \sim (\lambda + 2\mu)(Gh_0)^2 \sim 0.05$–$0.1$ eV Å^{-2}, for $h_0 \sim 1$ nm and $l = 2\pi G^{-1} \sim 60$ nm. This value is larger than typical interactions energies between a graphene layer and a SiO_2 substrate, or other materials, like water or ions, which may be trapped between graphene and the substrate [50]. Hence, we expect that, if graphene is pressed

Fig. 4. (Color online). Stresses along the line $(x, 0)$ for the periodic array of ripples analyzed in Fig. 1. Red: $\sigma_{xx}(x, 0)$. Green: $\sigma_{yy}(x, 0)$.

onto a corrugated SiO_2 substrate, the removal of that pressure will lead to the spontaneous formation of wrinkles. Note that the lowering of strains will actually reduce the effective gauge field acting on the electrons. On the other hand, the regions detached from the substrate can support low energy flexural modes, which can scatter electrons at finite temperatures [51,52].

4. Wrinkling of graphene layers: Suspended graphene samples

We now analyze the structural instabilities towards curved shapes, wrinkles, which can arise in suspended membranes under tension [53], see also Sec. VII in [13]. A stretched membrane with clamped ends will develop wrinkles if the applied tension is large enough [40]. This threshold arises from a balance between the bending energy and the applied tension [40]. Wrinkles will occur when the tension, $T \sim (\lambda + 2\mu)u_{xx}$ exceeds $\bar{\kappa}/l^2$, where l is the length of the stretched region. Hence, in graphene, stresses such that $u_{xx} \sim 10^{-2}$, will lead to wrinkles when l & 1 nm. The resulting deformation is periodic, with a wavelength, l_w, and amplitude, A, in the direction perpendicular to the applied strain given by [40]:

$$
\begin{aligned}
l_w &= 2\sqrt{\pi}\left(\frac{\bar{\kappa}}{T}\right)^{1/4} l^{1/2} \\
A &= \frac{\sqrt{2}}{\pi}\left(\frac{\lambda\bar{u}}{\lambda + 2\mu}\right)^{1/2} l_w .
\end{aligned}
\qquad (6)
$$

Typical wrinkles, calculated using Eq. (6) for a suspended region of length $l = 200$ nm, and an applied strain $\bar{u} = 2 \times 10^{-2}$ are shown in Fig. 5.

A suspended sheet with constant tension gives rise to a constant gauge field [27]. Electron scattering takes place at the boundaries between the region with and without tension, and the carriers propagate freely within the suspended region. Wrinkles modulate the strains in the direction of the applied tension and also in the direction perpendicular to it. As a result, an effective magnetic field is induced throughout the suspended region. This field is also shown in Fig. 5. Its average value scales as:

$$
\bar{B} \sim \frac{c\beta A^2 \Phi_0}{l_w^2 la} \sim \frac{c\beta\bar{u}\Phi_0}{la}. \qquad (7)
$$

Electronic transport in suspended graphene samples is expected to be close to the ballistic limit [54]. Hence, even the low fields induced by wrinkles may lead to observable effects.